

## Interparticle Potential and Drag Coefficient in Nematic Colloids

Jurij Kotar,<sup>1</sup> Mojca Vilfan,<sup>2</sup> Natan Osterman,<sup>1</sup> Dušan Babič,<sup>1</sup> Martin Čopič,<sup>1,2</sup> and Igor Poberaj<sup>1,2</sup>

<sup>1</sup>*Department of Physics, University of Ljubljana, Jadranska 19, SI-1000 Ljubljana, Slovenia*

<sup>2</sup>*J. Stefan Institute, Jamova 39, SI-1000 Ljubljana, Slovenia*

(Received 3 February 2006; published 23 May 2006)

Magneto-optic tweezers were used for measurements of liquid-crystal-mediated forces between spherical beads with tangential anchoring in thin nematic samples. Repulsive force, which results from the quadrupolar symmetry of defects around the immersed beads, decreases proportionally to  $1/x^6$ , with  $x$  being the bead separation. The velocity with which the particles are pushed apart also follows the same separation dependence. We thus find the effective drag coefficient  $\gamma_{\text{eff}}$  independent of  $x$  for surface-to-surface distances as small as 10% of the bead diameter.

DOI: [10.1103/PhysRevLett.96.207801](https://doi.org/10.1103/PhysRevLett.96.207801)

PACS numbers: 61.30.Gd, 47.57.J-, 87.80.Cc

Interactions between spherical particles immersed in a liquid crystal (LC) cause a rich variety of phenomena [1–5]. The origin of the observed effects lies in highly anisotropic long-range forces mediated by elastic deformations in the LC. Each particle immersed in the LC causes a distortion in the surrounding director configuration depending on the size and shape of the particle as well as on the strength and type of anchoring at the particle surface. Strong homeotropic anchoring results in a dipolar symmetry of the director field around the particle, whereas planar (tangential) anchoring conditions induce quadrupolar interactions between immersed beads. In latter case, the forces between two identical particles are either repulsive or attractive, depending on the orientation of the quadrupoles. Most of the experiments and theoretical considerations were made for homeotropic anchoring [6–10], and only recently Smalyukh *et al.* [11] reported on the first experimental observation of interactions between two particles with tangential anchoring conditions. They used optical tweezers in a planar bulk LC cell and have shown that, for fairly large bead separations ( $x > 4 \mu\text{m}$ , at a sphere diameter of  $3 \mu\text{m}$ ), the force decays proportional to  $x^{-6}$ , where  $x$  is the separation between the centers of the spheres. However, when using optical tweezers in liquid crystalline samples, we have shown previously [12] that the electric field of the trapping laser substantially alters the nematic director configuration around a trapped bead. This renders the obtained results hard to interpret. The reorientational effects can be reduced by choosing a low-birefringent liquid crystal or lowering the laser power [6,11]. An alternative approach to avoid the laser-induced LC distortions is to use magnetic particles along with a magnetic field for particle manipulation. This enables undistorted measurements of forces as well as effective drag coefficient of an immersed bead and its separation dependence.

We used combined magneto-optic tweezers for measuring the interparticle interactions and drag coefficient in nematic LC. The main advantage of this setup is that no distortions in the LC configuration appear due to the low

external magnetic field applied during the experiment. Even the largest field ( $\sim 10 \text{ mT}$ ) is too low to noticeably change the director configuration. Therefore, no requirements regarding the surrounding LC media are made, in contrast to the optical tweezers experiment.

The magneto-optic tweezers can operate in two different modes—the external magnetic field can induce either repulsive or attractive force between superparamagnetic beads. In our experiments, both modes were implemented, whereas the optical tweezers were used only for coarse positioning of the beads and were switched off during the measurement. This enabled us to measure the interparticle potential in a LC for a wide range of bead separations, most noticeably at small separations where experiments with optical tweezers become unreliable.

We used nematic liquid crystal 4-*n*-pentyl-4'-cyanobiphenyl (5CB, Aldrich) at room temperature. The particles were superparamagnetic spheres (Dynabeads, M-450 Epoxy, Dynalbiotech) with diameter  $2r_0 = 4.5 \mu\text{m}$ . Dried beads were suspended in the LC using a shaker and ultrasonic bath. For small magnetic fields ( $B < 10 \text{ mT}$ ), the magnetic dipole moment of a particle was proportional to the magnetic field  $m = m_0 \frac{\alpha}{3} B$ , with the coefficients  $m_0 = 1.204 \times 10^{-12} \text{ A m}^2$  and  $\alpha = 76/\text{T}$  [13]. The epoxy surface of the spheres induced tangential anchoring of the LC at the surface. This was confirmed with observations of the beads embedded in planar LC cells under a polarizing microscope [Fig. 1(a)]. Two point defects (boojums) at the poles of the sphere along the average director orientation  $\mathbf{n}_0$  are clearly visible. We also observed formation of bead chains at an angle of approximately  $\vartheta \approx 25^\circ\text{--}35^\circ$  with respect to the average director orientation [Fig. 1(b)]. Both are consistent with the quadrupolar nature of the director configuration observed previously [11,14].

The cells used in the experiment were prepared with silane treated glass plates (Aldrich 435708, 0.5% solution in water), which induced homeotropic alignment of liquid crystal molecules at the cell walls. A droplet of the LC-bead mixture was put on the glass slide and covered with a coated coverslip, which ensured a homogeneous distribu-

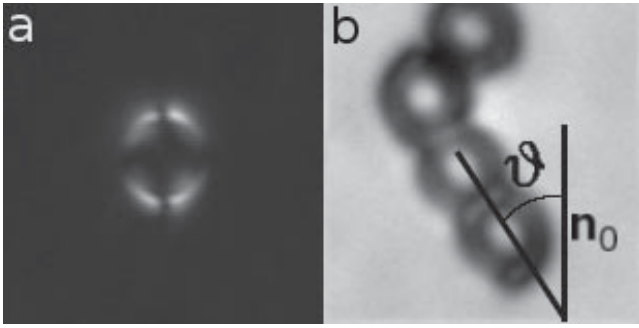


FIG. 1. (a) Colloidal particle ( $2r_0 = 4.5 \mu\text{m}$ ) immersed in nematic liquid crystal in a planar cell as seen under a polarizing microscope. Two boojums at the poles of the sphere along  $\mathbf{n}_0$  confirm tangential alignment of the director at the sphere surface and, thus, quadrupolar interparticle interaction. The boojums appearing very close to the sphere indicate fairly strong anchoring at the sphere surface. (b) Aggregation of particles was observed at an angle of approximately  $\vartheta \approx 25^\circ\text{--}35^\circ$  with respect to the average director orientation  $\mathbf{n}_0$ .

tion of particles. The cell was glued using a UV-curing glue. The thickness of the cell ( $l \approx 8 \mu\text{m}$ ) was less than twice the diameter of the spheres to prevent stacking of the beads on top of each other (Fig. 2, inset).

The measuring system was laser tweezers built around an inverted optical microscope (Zeiss, Axiovert 200M, Achroplan 63/0.9W objective) with the possibility of applying an external magnetic field by three orthogonal pairs of Helmholtz coils. The magnetic field perpendicular to the plane of the sample, in which the beads can move, induces

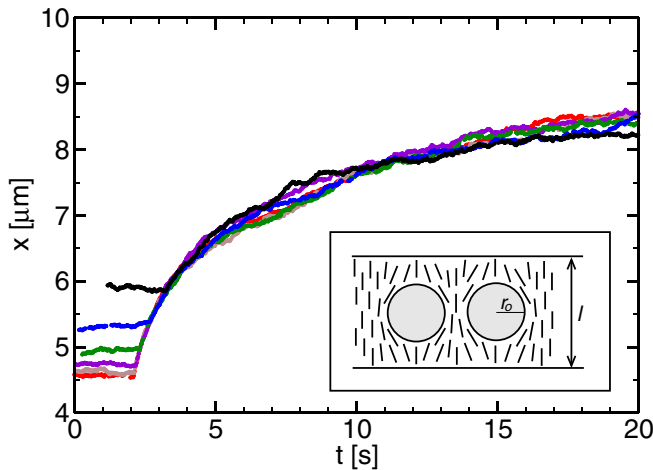


FIG. 2 (color online). Separation between the centers of the spheres  $x$  as a function of time  $t$ . The beads were brought into vicinity with an in-plane magnetic field (to several different initial separations  $x_0$ ) and then released. Quadrupolar symmetry due to the induced tangential anchoring in thin cells resulted in a repulsive force. Regardless of the initial separation, the beads followed the same trajectory. The inset shows a schematic director field configuration around two spheres inducing tangential anchoring in a homeotropic cell.

magnetic dipole moments in the spheres parallel to each other, and this results in a repulsive force. Attraction between induced dipoles in the particles can be obtained by a magnetic field rotating in the sample plane [15]. To prevent rotation of the bead pairs, the magnetic field was rotated back and forth for  $360^\circ$  with an effective frequency of 400 Hz.

The optical tweezers were generated with a Nd:YAG laser (Coherent, Compass 2500MN), where multiple traps were steered via acousto-optic deflectors (Intraaction, DTD-274HA6) and a beam steering controller (Aresis). The tweezers were used only for coarse positioning, i.e., for finding two beads and bringing them to a separation of around 10 microns, and were then switched off during the measurements.

The sample was illuminated with a halogen lamp and the beads were observed in bright field with a fast complementary metal-oxide semiconductor camera (PixelINK, PL-A741). The acquired images were analyzed using custom particle tracking software with a position accuracy of  $\approx 10 \text{ nm}$ .

To study the interparticle interactions, first the motion of free beads in the nematic cell was observed. A suitable pair of beads was found and brought to a separation of about 10 microns with optical tweezers. Then magnetic field inducing attractive interaction was used to move them to the initial position  $x_0$  and then switched off. When the field was switched off, the beads immediately started to drift apart due to quadrupolar interparticle interaction mediated by the surrounding liquid crystal. We measured particle trajectories  $x(t)$  for several different values of  $x_0$  ranging from 4.6 to  $5.9 \mu\text{m}$ . We observe that the particle separation as a function of time is independent of the initial separation  $x_0$ . This can be seen in Fig. 2 by the overlapping particle trajectories. The overlapping is extremely good for small  $x$ , whereas at larger separations ( $x \geq 6.5 \mu\text{m}$ ) the trajectories become strongly influenced by Brownian motion.

The overlapping of the trajectories indicates that the relaxation processes present in the nematic liquid crystal during the motion of the bead are fast enough to consider the director configuration around the beads as quasistationary. Such adiabatic behavior is not surprising, as typical relaxation times of the director field in several microns thick cells are of the order of 10 ms. This is much shorter than any characteristic time scale of the particle motion observed during measurements. Another important conclusion is that the parameters of the particle motion do not depend on the velocity. This is true even for very small initial separations ( $x_0 \approx 4.6 \mu\text{m}$ ). The motion of the particles is thus determined by the effective drag coefficient  $\gamma_{\text{eff}}$ , which includes the LC viscous drag, the impact of the cell walls, and the influence of LC distortions. The inertial term was neglected.

To obtain the effective drag coefficient  $\gamma_{\text{eff}} = F/v$  as a function of  $x$ , the interparticle force  $F(x)$  and their velocity

$v(x)$  have to be measured. In the first step, a set of experiments was performed where the LC-mediated repulsive interparticle force  $F$  was balanced with the attractive magnetic force  $F_B$ . The measurement was static, so all dynamic effects were excluded. Because of the low magnetic fields used in the experiment, pure interparticle force mediated by the LC was measured.

The experiments were performed in the following manner: First, the beads were brought together with sufficiently high magnetic field  $B$ . Electric current  $I$  through the coils was then reduced, and, for each value of  $I$ , the equilibrium position of the two particles was recorded. For small currents, where the bead separation  $x$  was as large as  $10 \mu\text{m}$ , Brownian motion prevailed. At that point, the electrical current and the magnetic field were increased again, and the whole cycle was repeated several times.

We observe that the equilibrium positions of the particles are the same at a given current when the magnetic field is increased or decreased. The absence of the hysteresis indicates that with varying particle separation the liquid crystal director configuration around the beads changes continuously and reversibly.

To determine the actual LC-mediated interparticle force, the balancing magnetic force had to be calibrated. Calibration was performed in two steps—first the functional dependence was determined and then the scaling factor was measured. The first part was performed in an isotropic medium. Measurements in water show that the repulsive force can be well described by  $F_{\text{rep}} = AI^2/x^4$ . The same force dependence was found also for attractive force  $F_{\text{att}} = \eta AI^2/x^4$ , with the factor  $\eta = 0.0091(1 \pm 0.13)$ . The measured forces are in agreement with the upper relations to within a few percent even at small bead separations ( $x \sim 2r_0$ ).

Knowing the dependence of force on the electric current and particle separation, the scaling coefficient  $A$  still had to be determined. This was done by observing the motion of the same bead pair as used in the actual force measurements in the LC. Any error due to possible variations in the bead susceptibility was thus excluded. The procedure was as follows: First, the particles were brought to contact with an in-plane magnetic field; then the field was switched off and the particles drifted apart (Fig. 3, A). When Brownian motion prevailed, the perpendicular magnetic field was switched on, which resulted in an additional repulsive force (Fig. 3, B). The latter part of the trajectory can be well described if  $x(t)$  dependence is calculated from

$$F_{\text{rep}} = \frac{AI^2}{x^4} = \gamma \frac{\dot{x}}{2}, \quad (1)$$

where the inertial term is neglected. The factor  $1/2$  comes from the fact that for symmetric interactions the change in the separation  $x$  is twice the displacement of one sphere. The coefficient  $\gamma$  in Eq. (1) is given by the Stokes-Einstein relation  $\gamma = k_B T/D$ , where  $k_B$  is the Boltzmann constant,

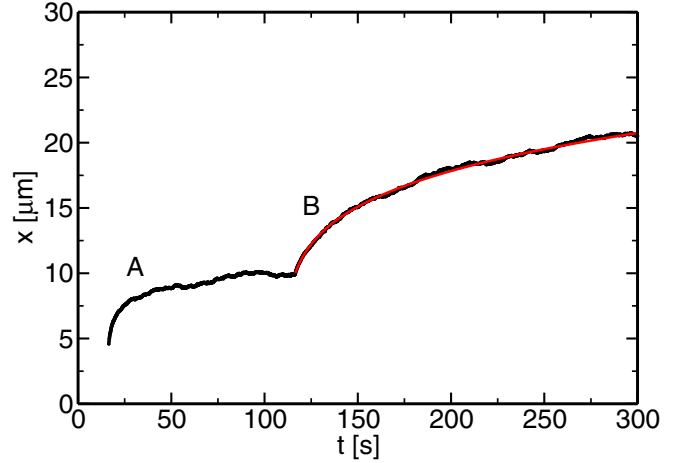


FIG. 3 (color online). Calibration of the magnetic force between two superparamagnetic beads in nematic liquid crystal under external magnetic field. The beads were brought together with an in-plane magnetic field, then released to drift apart (A). When Brownian motion prevailed, an out-of-plane magnetic field was applied to cause additional repulsive force (B). This part of the trajectory can be well described by theoretical prediction (solid line) and the scaling coefficient of the magnetic force obtained. See text for details.

$T$  is the temperature, and  $D$  is the diffusion coefficient. The coefficient  $\gamma$  is obtained separately by analyzing the Brownian motion of a single particle [16,17]. From the obtained value  $\gamma = 4.2(1 \pm 0.03) \text{ pN s}/\mu\text{m}$ ,  $D$  can be calculated and is in very good agreement with the diffusion coefficient obtained previously [17]. From Eq. (1), the relation

$$x(t) = \left( \frac{10AI^2}{\gamma} (t - t_0) \right)^{1/5} \quad (2)$$

is obtained and fitted to the experimental data (Fig. 3, B). The best fit to the data yields the value for the calibration factor with an accuracy of approximately 10%.

Knowing the magnetic force at a given electrical current and bead separation, the colloidal force mediated by the nematic liquid crystal can be calculated. The obtained repulsive force  $F$  as a function of normalized particle separation  $x/2r_0$  is shown in Fig. 4. The force can be well described using theoretical model for quadrupolar interaction between two particles [8]:

$$F = \frac{4\pi W^2 r_0^8}{Kx^6} \left( 1 - \frac{Wr_0}{56K} \right) = \frac{C}{(x/2r_0)^6}, \quad (3)$$

where  $W$  is the anchoring energy coefficient at the sphere surface and  $K$  is the Frank elastic constant in one-constant approximation. The best fit of Eq. (3) to the measured data yields  $C = 4.69(1 \pm 0.18) \text{ pN}$ .

Returning to the dynamic measurements, where the beads drift apart only due to forces mediated by the liquid

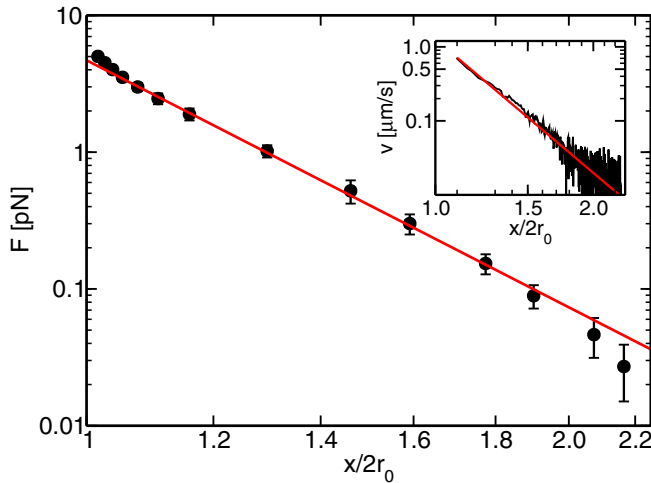


FIG. 4 (color online). Force between two beads immersed in a nematic liquid crystal with tangential anchoring (circles). The force in thin cells is repulsive and follows the power law  $F \propto 1/x^6$  (solid line) for a wide range of particle separation  $x$  down to  $x/2r_0 = 1.05$ . The solid line is the best fit of Eq. (3) to the data. Inset: Velocity of a particle  $v$  as a function of normalized interparticle separation  $x/2r_0$ . The solid line is the best fit of  $v \propto 1/x^6$ .

crystal, the velocity of a particle  $v$  as a function of interparticle separation can be calculated. The inset in Fig. 4 shows the calculated velocity  $v$  as a function of normalized particle separation  $x/2r_0$ . Within the experimental error, the obtained velocity can be well fitted with  $v = C_1/(x/2r_0)^6$  (solid line in Fig. 4, inset) yielding coefficient value  $C_1 = 1.25 \mu\text{m/s}$ .

Since both interparticle force  $F$  and velocity  $v$  of a moving bead follow  $1/x^6$  dependence, we find that, within experimental error, the effective drag coefficient  $\gamma_{\text{eff}} = F/v$  is independent of the separation between the particles for  $x > 4.9 \mu\text{m}$ . The obtained value  $\gamma_{\text{eff}} = 3.8(1 \pm 0.20) \text{ pNs}/\mu\text{m}$  is in agreement with the drag coefficient obtained from the analysis of single particle Brownian motion.

To conclude, we have used magneto-optical tweezers to measure the force in a nematic liquid crystal between two particles inducing tangential anchoring. We find that the force mediated by the liquid crystal follows the  $1/x^6$  dependence in a wide range of interparticle separations from  $x \sim 2r_0$  to  $x \sim 5r_0$  ( $10 \mu\text{m}$ ). Combining static and dynamic measurements, the effective drag coefficient  $\gamma_{\text{eff}} = F/v$  was determined and within experimental error found to be independent of the particle separation for  $x >$

$4.9 \mu\text{m}$ , which means for surface-to-surface distance as small as 10% of the bead diameter.

This behavior is surprising because significant distortions in the director field around the beads are observed, which could result in a separation dependent drag coefficient. Apparently, the previously observed deviation from the power law [6] is due to externally induced distortions. The combined magneto-optical tweezers have proven to be successful for colloidal studies in liquid crystals, especially as both repulsive and attractive external force can be generated without any measurable effect of the external fields on the director configuration.

- [1] P. Poulin, H. Stark, T.C. Lubensky, and D.A. Weitz, *Science* **275**, 1770 (1997).
- [2] J.C. Loudet and P. Poulin, *Phys. Rev. Lett.* **87**, 165503 (2001).
- [3] H. Stark, *Phys. Rep.* **351**, 387 (2001).
- [4] J. Yamamoto and H. Tanaka, *Nature (London)* **409**, 321 (2001).
- [5] I.I. Smalyukh, S. Chernyshuk, B.I. Lev, A.B. Nych, U. Ognysta, V.G. Nazarenko, and O.D. Lavrentovich, *Phys. Rev. Lett.* **93**, 117801 (2004).
- [6] I.I. Smalyukh, A.N. Kuzmin, A.V. Kachynski, P.N. Prasad, and O.D. Lavrentovich, *Appl. Phys. Lett.* **86**, 021913 (2005).
- [7] M. Yada, J. Yamamoto, and H. Yokoyama, *Phys. Rev. Lett.* **92**, 185501 (2004).
- [8] R.W. Ruhwandl and E.M. Terentjev, *Phys. Rev. E* **55**, 2958 (1997); **56**, 5561 (1997).
- [9] O. Guzmán, E.B. Kim, S. Grollau, N.L. Abbott, and J.J. de Pablo, *Phys. Rev. Lett.* **91**, 235507 (2003).
- [10] J. Fukuda, H. Stark, M. Yoneya, and H. Yokoyama, *Phys. Rev. E* **69**, 041706 (2004).
- [11] I.I. Smalyukh, O.D. Lavrentovich, A.N. Kuzmin, A.V. Kachynski, and P.N. Prasad, *Phys. Rev. Lett.* **95**, 157801 (2005).
- [12] I. Mušević, M. Škarabot, D. Babič, N. Osterman, I. Poberaj, V. Nazarenko, and A. Nych, *Phys. Rev. Lett.* **93**, 187801 (2004).
- [13] V. Blicke, D. Babič, and C. Bechinger, *Appl. Phys. Lett.* **87**, 101102 (2005).
- [14] P. Poulin and D.A. Weitz, *Phys. Rev. E* **57**, 626 (1998).
- [15] B.A. Grzybowski, H.A. Stone, and G.M. Whiteside, *Nature (London)* **405**, 1033 (2000).
- [16] J.C. Crocker and D.G. Grier, *J. Colloid Interface Sci.* **179**, 298 (1996).
- [17] J.C. Loudet, P. Hanusse, and P. Poulin, *Science* **306**, 1525 (2004).